



Relations between microstructure and hardness of plain carbon steels using eddy current technique

Isadora Costa, Christophe Mesplont, Jeremie Bouquerel, Jean-Bernard Vogt

► To cite this version:

Isadora Costa, Christophe Mesplont, Jeremie Bouquerel, Jean-Bernard Vogt. Relations between microstructure and hardness of plain carbon steels using eddy current technique. 5th International Conference on Manufacturing, Material and Metallurgical Engineering, Mar 2020, Osaka, Japan. 10.1088/1757-899x/859/1/012005 . hal-02530527

HAL Id: hal-02530527

<https://hal.univ-lille.fr/hal-02530527>

Submitted on 22 Jun 2020

HAL is a multi-disciplinary open access archive for the deposit and dissemination of scientific research documents, whether they are published or not. The documents may come from teaching and research institutions in France or abroad, or from public or private research centers.

L'archive ouverte pluridisciplinaire **HAL**, est destinée au dépôt et à la diffusion de documents scientifiques de niveau recherche, publiés ou non, émanant des établissements d'enseignement et de recherche français ou étrangers, des laboratoires publics ou privés.

PAPER • OPEN ACCESS

Relations between microstructure and hardness of plain carbon steels using eddy current technique

To cite this article: Isadora M. O. A. Costa *et al* 2020 *IOP Conf. Ser.: Mater. Sci. Eng.* **859** 012005

View the [article online](#) for updates and enhancements.

Relations between microstructure and hardness of plain carbon steels using eddy current technique

Isadora M. O. A. COSTA^{1,2}, Christophe MESPLONT², Jérémie BOUQUEREL¹, Jean-Bernard VOGT^{1*}

¹ Univ. Lille, CNRS, INRAE, Centrale Lille, UMR 8207 - UMET - Unité Matériaux et Transformations, F-59000 Lille, France

² Bekaert NV, Bekaertstraat 2, 8550 Zwevegem, Belgium

* jean-bernard.vogt@univ-lille.fr

Abstract. Heat-treatments were carried out on carbon steels ranging from 0.03 to 0.78 wt%C, in order to produce various ferrite-pearlite microstructures. The specimens were characterized by metallographic examinations and microhardness measurements. A clear dependence was found between microstructure characteristics and eddy current outputs measured by means of an electromagnetic sensor: resistance was observed to increase, while inductive reactance decreased in the order of pearlite and ferrite microstructures, and with decreasing interlamellar spacing of pearlite. These components are related to the electrical resistivity and magnetic permeability of the steels. The potentiality of this technique was highlighted for monitoring phase proportions, quantitatively assessing pearlite interlamellar spacing, giving also information about mechanical properties, such as hardness. It reveals the great potential of eddy current testing as a reliable non-destructive tool for metallurgical and mechanical characterization of carbon steels.

1. Introduction

The knowledge and adequate control of the microstructural and mechanical properties of steels are a part of a general approach for improving performance of manufacturing process and enhancing final product quality. In this context, non-destructive techniques have attracted considerable interest for the evaluation of material characteristics and monitoring in-service degradation of components. Among the various non-destructive techniques, eddy current testing is a widely used electromagnetic method for discontinuities and defects detection, corrosion damage inspection and coating thickness measurement in conductive materials [1,2]. More recently, eddy current method has been developed for material characterization, due to its sensitivity to material's permeability and resistivity variations [3-5]. Indeed, magnetic and electrical properties of ferromagnetic materials are known to be altered by their chemical composition [6,7], microstructure [8-11], and to some extent, by their residual stresses [12,13].

In the present work, eddy current method was used to investigate the influence of metallurgical characteristics on the electrical resistivity and magnetic permeability of carbon steels. Heat treatments were performed to produce various ferrite-pearlite microstructures. Microstructural observation and microhardness tests were conducted on the thermally treated carbon steels. Eddy current testing was



carried out using an electromagnetic sensor. The objective of this study is to evaluate the feasibility of eddy current testing for measuring and monitoring carbon steel characteristics.

2. Experimental procedure

2.1. Materials and heat treatments

The samples examined in this study were obtained from carbon steels with carbon content varying from 0.03 to 0.78 wt%C, the compositions of which are given in Table 1. In order to produce specimens with different types of grains, ferrite and pearlite, the steels with various amounts of carbon were austenitized at 950°C and cooled at 580°C. Group A consists of different batches of steels with different ferrite/pearlite fractions. It is worth to mention that heat treatments were carried out at fast cooling rates, which configures a non-equilibrium transformation. As a result, the pearlite volume fraction obtained for each steel composition was higher than it would be obtained in an equilibrium condition. Group B includes entirely pearlitic samples with various lamellar spacings obtained from a 0.78 wt%C steel. Aiming at obtaining different interlamellar spacings, the samples were austenitized at 950°C and cooled at six different temperatures ranging from 540 to 640°C.

2.2. Microstructural and mechanical characterization

Metallographic preparation of the heat-treated steel samples involved abrasive cutting, mounting, followed by grinding and polishing using successively finer water-based diamond suspensions. The microstructural observations were performed by light optical microscopy (LOM) and scanning electron microscopy (SEM). Prior-austenite grain sizes and volume fractions of phases were measured on randomly selected fields in the LOM, using the image analysis software ImageJ/Fiji. Grain sizes were measured by the intercept method after thermal etching with alkaline sodium picrate solution to reveal austenite grain boundaries [14,15], while the quantification of phase fraction was done by phase-contrast image analysis after color etching with 3% Nital and 10% potassium metabisulfite solution [14]. The interlamellar spacing was measured on SEM images using the Underwood method, by which the mean true interlamellar spacing could be randomly estimated according to its intersection procedure [16]. Prior-austenite grain sizes were considered approximately equal for all samples, varying from 20 to 40 μm in diameter. One-way analysis of variance (ANOVA) was carried out to confirm that the differences in the estimated phase fraction and interlamellar spacing values between the samples were statistically significant. Mechanical characteristics were determined via Vickers microhardness measurements.

Table 1. Summary of the chemical composition, various heat treatments, pearlite volume fraction (P) and average interlamellar spacing (\bar{S}), and microhardness values of the investigated steels

AISI designation	Chemical composition (wt%)				Heat treatments	P (%)	\bar{S} (nm)	Vickers hardness number
	C	Mn	Si	Fe				
Group A								
1000	0.03	0.15	0.01	Bal.	Austenitizing at 950°C Cooling at 580°C	0	—	112
1020	0.20	0.73	0.26	Bal.		28.7	243 ± 68	170
1035	0.35	0.61	0.21	Bal.		78.3	196 ± 21	209
1050	0.50	0.59	0.21	Bal.		94.7	157 ± 16	266
1055	0.52	0.61	0.21	Bal.		95.8	156 ± 13	272
1060	0.58	0.61	0.19	Bal.		98.1	153 ± 16	295
1065	0.65	0.61	0.18	Bal.		99.1	155 ± 30	317
1080	0.78	0.59	0.24	Bal.		100	126 ± 20	354
Group B								
1080	0.78	0.59	0.24	Bal.	Cooling at 540°C	100	95 ± 9	374
1080	0.78	0.59	0.24	Bal.	Cooling at 560°C	100	103 ± 12	370

1080	0.78	0.59	0.24	Bal.	Cooling at 580°C	100	126 ± 20	354
1080	0.78	0.59	0.24	Bal.	Cooling at 600°C	100	129 ± 22	350
1080	0.78	0.59	0.24	Bal.	Cooling at 620°C	100	153 ± 27	328
1080	0.78	0.59	0.24	Bal.	Cooling at 640°C	100	185 ± 37	322

2.3. Eddy current testing

Eddy current testing is based on the principles of the electromagnetic induction. It consists of an alternating current generator that applies an alternating voltage to a coil circuit. A current flows through it, which causes an alternating magnetic field to develop around the coil, in phase with the voltage and the primary current. If a conductive material is brought into the proximity to this changing magnetic field, eddy currents are induced into it. Eddy currents cause a secondary flux to develop into the material in opposite polarity to the primary flux. A change in the overall net magnetic flux results in a changing of coil impedance, composed by a resistive component and an inductive term, as indicated:

$$Z = \sqrt{R^2 + X_L^2} \quad (1)$$

where the resistance R and the inductive reactance X_L represent, respectively, the real and imaginary parts of the coil's impedance Z in ohms. Impedance changes depend on the magnitude of eddy currents, which are a function of electrical conductivity and magnetic permeability of the material, beyond parameters such as test frequency and fill-factor. Thus, eddy current testing can be assumed as an indirectly response of microstructure characteristics of conductive materials. In this study, conventional coil arrangement connected through an oscillator circuit and an amplifier to a data acquisition computer was employed. Tests were performed at room temperature and at a fixed test frequency, in the way that electrical resistivity and magnetic permeability were the only effective parameters affecting the material response to the induced current. The impedance plane is the convention for representing eddy current signals, and voltage signal variations were used to display impedance variations of the coil.

3. Results and discussions

3.1. Ferrite-pearlite structures: effect of carbon content

Typical microstructures of the heat-treated steel samples are shown in optical micrographs of Figure 2. The ultra-low carbon 1000 steel was used to produce a fully ferritic microstructure of α -phase, which is a solid solution of carbon in iron. Hypoeutectoid steels were used for producing ferrite-pearlite structures with pearlite fractions varying from 28.7 to 99.1%. In these structures, a network of proeutectoid ferrite (bright regions) is observed along the grain boundaries surrounding areas of pearlite (dark regions), which is a constituent consisted of alternate lamellae of eutectoid α ferrite and cementite (Fe_3C) phases. The eutectoid 1080 steel exhibited a fully pearlitic microstructure.

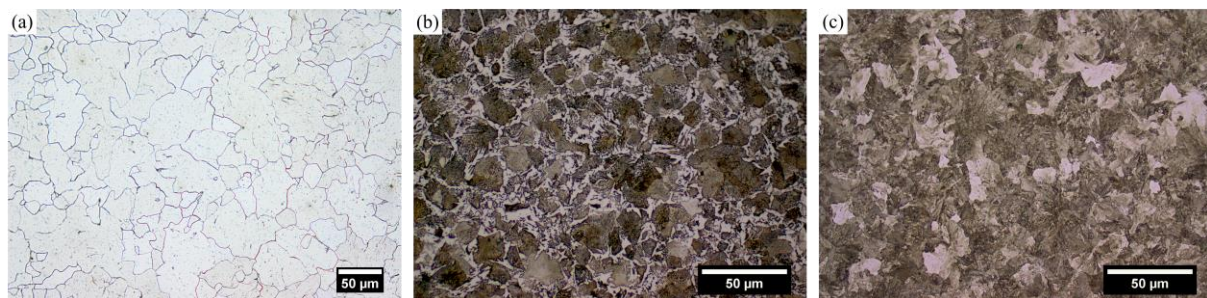


Figure 1. Optical micrographs of (a) ferrite, (b) ferrite-pearlite and (c) pearlite structures

Hardness was observed to increase linearly with the increase of carbon content. As the pearlite fraction increases, the proportion of cementite, which is a relatively hard phase, also increases and the hardness of the steel rises accordingly. Figure 2-a shows the impedance changes with respect to the Vickers hardness values of the ferrite-pearlite microstructures. Impedance values decreased with the increase of carbon content, and so with the increase of the Vickers hardness. The impedance plane that includes the resistance and the inductive reactance components is shown in Figure 2-b. Inductive reactance values were observed to decrease, while resistance increased with increasing carbon content.

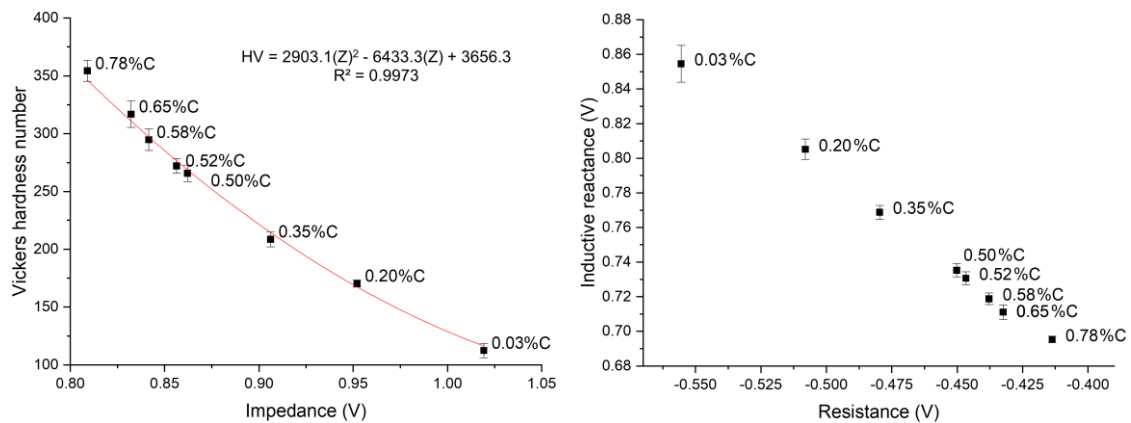


Figure 2. Relations between hardness and eddy current outputs (left); (b) impedance plane of plain carbon steels (right)

3.2. Pearlite structures: influence of pearlite interlamellar spacing

Aiming at evaluating more clearly the role of the spacing of pearlite lamellae, fully pearlitic samples were produced by varying the temperature at which austenite is transformed. A decrease in the transformation temperature was observed to refine the interlamellar spacing between ferrite and cementite lamellae, as observed in Figure 3. In the SEM images, the dark regions are the α -phase that occurs both in the pearlite and in the simple ferrite grains, while the Fe_3C cementite is white and sticks out of the ferrite matrix. Narrower \bar{S} means more interfaces between ferrite matrix and cementite lamellae, leading to an increase in hardness that correlated well with the decrease in impedance values observed in Figure 4-a. In Figure 4-b, the complex impedance plane shows that, inductive reactance values decreased with decreasing interlamellar spacing of pearlite, while resistance values increased.

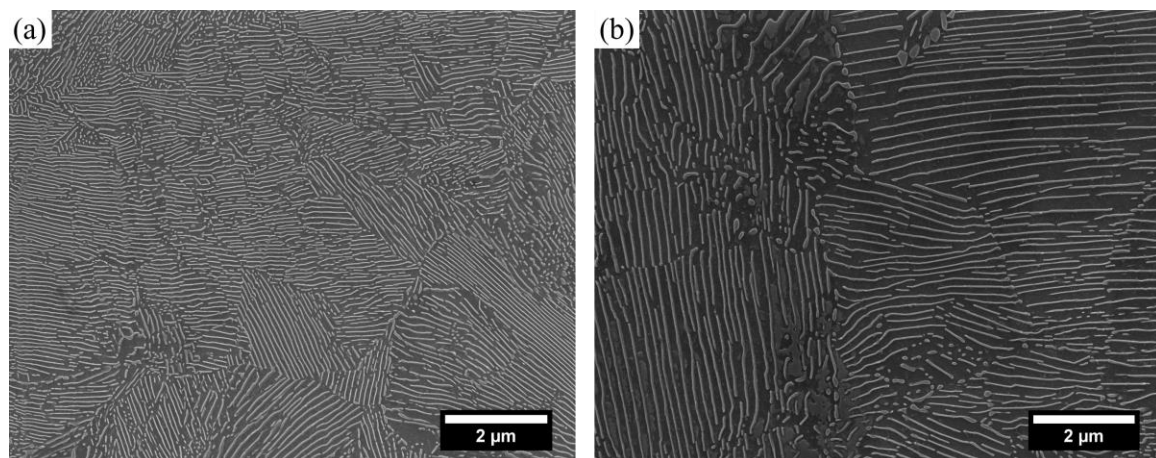


Figure 3. SEM images of 1080 steels cooled at (a) 540°C (\bar{S} =95 nm), and (b) 640°C (\bar{S} =185 nm)

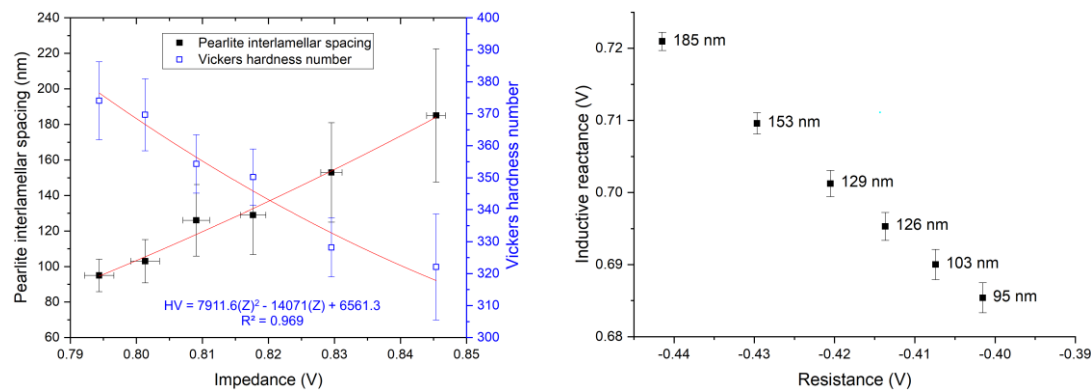


Figure 4. Relations between interlamellar spacing, hardness and eddy current outputs (left); impedance plane of eutectoid steels (right)

3.3. Assessment of the effect of microstructure on physical properties of carbon steels

The potentiality of eddy current testing was highlighted to distinguish the different arrangements of ferrite-pearlite microstructures and estimate pearlite interlamellar spacing, giving also information about hardness of thermally treated carbon steels. Carbon steels could be characterized by measuring changes in inductive reactance and effective resistance of an electromagnetic sensor operating at low frequencies. These components are related, respectively, to the magnetic permeability and electrical resistivity of the ferromagnetic steels [1,2]. The overall electromagnetic behavior in a multiphase structure was observed to be a function of their different microstructural features. The resistance increased while inductive reactance decreased with carbon content due to the different amounts of pearlite in the steels. It was also observed an increase of resistance and a decrease of inductive reactance with the decrease of pearlite interlamellar spacing. These effects were attributed to the propagation and nucleation processes of magnetic domain walls, and to the electrons mobility into the crystalline microstructure. The presence of a lamellar carbide network influenced the magnetic response between the various microstructures, as it represents effective pinning sites that hinder domain wall motion [4,17-19]. Moreover, cementite layers can act as scattering centers for electrons, which would lead to the increase of steel resistivity [11]. For each material, the mechanically harder specimens exhibited higher resistance and lower inductive reactance, indicating that hardness can be readily measurable by eddy current testing.

4. Conclusions

From the study to evaluate the influence of microstructure and hardness on the electrical resistivity and magnetic permeability of carbon steels by means of eddy current measurements, it can be concluded:

1. Resistance (electrical resistivity) was observed to increase while inductive reactance (magnetic permeability) decreased in the order of pearlite, ferrite-pearlite and ferrite microstructures, and with a narrower interlamellar spacing of fully pearlitic microstructures.
2. Quantitative linear correlations were obtained between microstructure features, hardness and eddy current outputs. Hence, the results of this research reveal the great potential of eddy current technique to be used as a reliable non-destructive tool for characterization of carbon steels.

References

- [1] C.J. Hellier, Handbook of nondestructive evaluation, second ed., McGraw-Hill, New York, 2003
- [2] J. García-Martín, J. Gómez-Gil, E. Vázquez-Sánchez, Sensors. 11 (2011) 2525–2565.
- [3] M.K. Devine, JOM. 44 (1992) 24–30.
- [4] O. Saquet, J. Chicois, A. Vincent, Mater. Sci. Eng. A. 269 (1999) 73–82.

- [5] C. Davis, M. Strangwood, A. Peyton, *Ironmaking Steelmaking*. 38 (2011) 510–517.
- [6] D. Mercier, J. Lesage, X. Decoopman, D. Chicot, *NDT&E INT.* 39 (2006) 652–660.
- [7] M.S. Amiri, M. Kashefi, *NDT&E INT.* 42 (2009) 618–621.
- [8] F. Rumiche, J.E. Indacochea, M.L. Wang, *JMEP.* 17 (2008) 586–593.
- [9] S. Konoplyuk, *NDT&E INT.* 43 (2010) 360–364.
- [10] S. Ghanei, M. Kashefi, M. Mazinani, *Mater. Des.* 50 (2013) 491–496.
- [11] L. Zhou, J. Liu, X.J. Hao, M. Strangwood, A.J. Peyton, C.L. Davis, *NDT&E INT.* 67 (2014) 31–35.
- [12] W. Ricken, H.C. Schoenekess, W.J. Becker, *Sens. Actuator A-Phys.* 129 (2006) 80–85.
- [13] B. Cao, T. Iwamoto, *Steel Res. Int.* 87 (2017) 1–10.
- [14] L.B. Bramfitt, O.A. Benschoter, *Metallographer's guide: Practices and procedures for irons and steels*, ASM International, 2002.
- [15] ASTM E112-13 Standard test methods for determining average grain size, ASTM International, West Conshohocken, PA, 2013.
- [16] G.F. Vander Voort, A. Róosz, *Metallography.* 17 (1984) 1–17.
- [17] L. Clapham, C. Jagadish, D.L. Atherton, *Acta Metall. Mater.* 39 (1991) 1555–1562.
- [18] S.M. Thompson, B.K. Tanner, J. Magn. Magn. Mater. 123 (1993) 283–298.
- [19] J.W. Byeon, S.I. Kwun, *Mater. Trans.* 44 (2003) 2184–2190.